Food Chemistry: X 14 (2022) 100304

Contents lists available at ScienceDirect

Food Chemistry: X

journal homepage: www.sciencedirect.com/journal/food-chemistry-x

Haem-mediated protein oxidation affects water-holding capacity of beef during refrigerated storage

Jun Liu [a], Dunhua Liu [a,b,*], Anran Zheng [a], Qin Ma [b]

[a] School of Agriculture, Ningxia University, 750021 Yinchuan, China
[b] School of Food & Wine, Ningxia University, 750021 Yinchuan, China

ARTICLE INFO

Keywords:
Beef
Water holding capacity
Haem
Lipid oxidation
Protein oxidation

ABSTRACT

Haem is considered to be a potential producer of meat oxidation and the effect of its mediated oxidation on the water holding capacity (WHC) of beef is not yet clear. This work investigated the interrelationships between haem, protein and lipid oxidation, and WHC in beef during refrigerated storage. The increase in juice loss during storage ($p < 0.05$) indicates a reduction in WHC. Haem was oxidised, resulting in its structural disruption and an increase in the proportion of random coil in the protein secondary structures ($p < 0.05$). Extractable haem iron content was decreased and non-haem iron content was increased ($p < 0.05$), indicating the degradation of haem and the release of iron during storage. The levels of lipid and protein oxidation products significantly increased throughout the storage time ($p < 0.05$). Furthermore, Spearman analysis verified significant correlations between these changes. In conclusion, these processes are mutually reinforcing and may exacerbate muscle juice loss.

1. Introduction

Water-holding capacity (WHC) is defined as the ability of fresh meat to retain its water, which is a quality attribute of meat products due to its great impacts on fresh weight, sensory acceptability (colour, juiciness and texture) and economic benefits (Zhang, et al., 2019; Zheng, et al., 2018). The majority of water in muscle is held within the myofibrillar protein network and depends on electrostatic forces, osmotic forces, and capillary forces to bind tightly to the myofibrillar charged hydrophilic groups (Pearce, et al., 2011). Consequently, changes in the structure of the muscle fibres and their spatial arrangement during ageing may affect the WHC of the meat. There is evidence that oxidative modification may modify amino acid side chains, alter the hydrophilic and hydrophobic areas of the myofibrils proteins (MP) and the interaction with structural elements within the sarcomere and between the myofibrils, affect protein cross-linking and protein net charges, and thereby influence the structure of muscle fibres and their spatial arrangement (Bao & Ertbjerg, 2019). Reactive oxygen species (ROS) can be produced during normal metabolism of muscle, and accumulation of ROS can be induced by metal ions and fat oxidation products, when ROS exceeds the defense of endogenous antioxidant capacity, ROS may cause the oxidative modification of myofibrillar proteins (Zhang, et al., 2019). Iron ions, a strong oxidant, can promote protein and lipid oxidation through numerous mechanisms (Wang, et al., 2020), and has received interest in terms of their potential role and significance in meat protein and lipid oxidation.

Iron is mainly carried in the muscle as haemoglobin (Hb) and myoglobin (Mb), of which Hb consists of four polypeptide chains with each chain containing one heme group, the latter containing an iron atom that is coordinated within the heme ring. Mb, a monomeric heme protein, consists of a globin moiety plus a porphyrin heme, with properties similar to Hb (Richards, et al., 2007; Thiansilakul, et al., 2012; Zhang, et al., 2021). During muscle storage, hemin (ferric heme) can be separated from the bead protein, and the released heme and iron have been recognized as major catalysts for protein and lipid oxidation (Grunwald & Richards, 2006). The essence of haem autoxidation is the conversion of ferrous Mb (or Hb) to ferric metmyoglobin, the further conversion of oxymyoglobi (OxyMb) to metmyoglobin (MetMb), and the "Fenton reaction" converting peroxyl radicals to hydroxyl radicals (•OH) (Thiansilakul, et al., 2012). Many investigators have studied Hb and Mb oxidation systems in meat. For example, Hanan and Shaklai (1995) found that H_2O_2-generated myoglobin radical caused cross-linking of myosin in rabbit leg muscles;) The iron-catalyzed oxidizing and metmyoglobin-oxidizing system induced the cross-linking of yak muscle myofibrillar protein myosin heavy chain (Wang, et al., 2020); Richards et al., (2004) reported the released of iron from hemoglobin-mediated lipid oxidation in cod muscle. In summary, the process of

* Corresponding author at: No. 489, Mount Helan West Road, Xixia District, Yinchuan City 750000, Ningxia Hui Autonomous Region, China.
E-mail address: ldh320@nxu.edu.cn (D. Liu).

https://doi.org/10.1016/j.fochx.2022.100304
Received 6 March 2022; Received in revised form 31 March 2022; Accepted 6 April 2022
Available online 9 April 2022

meat autoxidation is accompanied by a heme oxidation system-dependent effect.

Iron is the most abundant trace metal in beef, and the susceptibility of fresh beef to iron-mediated reactions depends on haem type (Rhee & Ziprin, 1987; Valenzuela, et al., 2009). More specifically, there are no reports about the effects of haem structure and inorganic iron on myofibrillar proteins and lipid oxidation during beef ageing, or on meat quality. Research in this area is necessary to clarify whether haem (myoglobin and haemoglobin) is an active perpetrator, and improve the degree of protein oxidation and WHC in beef. Therefore, the study aimed to determine the concentrations, morphology and structure of Hb and Mb durig postmortem storage of fresh beef and the release of metallic iron, and their relationshipswith lipid oxidation, MP oxidation and WHC.

2. Materials and methods

2.1. Materials

Eight male Chinese yellow cattle (Qinchuan cattle) with ages of 1–2 years and live weights of 400 ± 20 kg were humanly killed at Ningxia Yitai Herding Co. according to the guidelines of the Canadian Council on Animal Care. Following cattle exsanguinations, muscle samples from longissimus dorsi muscles were immediately obtained and placed in a foam box filled with ice packs and deliveried to the laboratory within 3 h. The muscle samples were cut into pieces with an average weight of 100 ± 2.5 g, and 40 randomly selected muscles were then assigned to five groups. The samples were placed on plastic trays and stored at 4 °C for 0, 1, 2, 4 and 6 days (0 d, 1 d, 2 d, 4 d and 6 d). Each group of samples was divided into two parts, fresh samples were used for meat quality analysis, and the remaining samples were immediately frozen in liquid nitrogen and stored at −80 °C (Chen, et al., 2021).

2.2. Evaluation of beef quality

The color values of meat were measured on the surface of meat samples using a CR-410 hand-held Chroma Meter (Minolta Co., Ltd., Suita, Osaka, Japan) within five copies at different locations of each sample, with six replicates per storage time. For pH analysis, a portable pH meter with a puncture electrode (Testo 205 AG; Lenzkirch, Germany) was used.

Purge loss (PL), drip Loss (DL) and centrifuging loss (CL) were measured using the method of Chen, et al. (2015) and Li, et al. (2018). The PL was determined by calculating the percentage of weight loss during storage. The initial weight of each steak piece was recorded, and 24 h after storage at 4 °C, samples removed from the trays were immediately tissue dried and weighed again. Muscle with a weight of approx. 10 g was hung in a sealed Honikel bag for 24 h at 4 °C. The results were calculated as the difference in weight before and after hanging, with DL expressed as a percentage of the weight before hanging. 2 g of meat was wrapped in filter paper and centrifuged at 1,500 × g for 5 min at 4 °C. CL was measured as weight loss during centrifugation, with CL expressed as a percentage of initial meat weight.

2.3. Moisture distribution in muscle by low-field NMR relaxometry (LF-NMR)

A muscle sample of 2.0 ± 0.2 g was taken along the direction of muscle fiber and placed in a 15 mm diameter NMR tube for measurements. The measurements were carried out on a Benchtop Pulsed NMR analyzer (NMI20, Shanghai Niumag Electronic Technology Co., Shanghai, China) using the Carr-Purcell-meiboom-Gill (CPMG) pulse sequence, proton resonance frequency SF of 18 MHz, offset frequency of 382.241 65 kHz, 90° and 180° pulse times of 16 μs and 33 μs, respectively. A recycle delay of 100 μs and 16 scans was used for a recording of 2000 echo maxima at 25 °C. The data were analysed using the instrument's software (NIUMAG ver. 1.0, Shanghai Niumag Electronic Technology Co., Shanghai, China) and the transverse relaxation spectrum (T_2) obtained. The abscissa of the spectrum was the transverse relaxation time, and the ordinate was the amplitude of the hydrogen proton signal (Li, et al., 2018).

2.4. Measurement of Mb concentration

A minced muscle sample (5 g) was mixed with 20 mL of cold 0.04 M phosphate buffer, pH 6.8, and then homogenized at 3,000 rpm for 60 s using a Waring blendor (FJ300-SH, Shanghai Standard Model Co., Ltd., Shanghai, China). The resulting sample was centrifuged at 4,500 × g for 30 min at 4 °C, and the supernatant was filtered with Whatman No. 1 filter paper. Mb concentration was determined by absorbance at 503, 525, 557 and 582 nm using an UV visible spectrophotometer (UV-9000S Metash Instruments co, Ltd, Shanghai, China). The proportions of three myoglobin forms, deoxymyoglobin (DeoMb), oxymyoglobin (OxyMb) and metmyoglobin (MetMb) were calculated using a modified Krzywicki's equation (Tang, et al., 2004) as follows:

$$\mathrm{DeoMb} = C_{\mathrm{DeoMb}}/C_{\mathrm{Mb}} = -0.534R_1 + 1.594R_2 + 0.552R_2 - 1.329$$

$$\mathrm{OxyMb} = C_{\mathrm{OxyMbb}}/C_{\mathrm{Mb}} = 0.722R_1 - 1.432R_2 - 1.659R_2 + 2.599$$

$$\mathrm{OxyMb} = C_{\mathrm{OxyMb}}/C_{\mathrm{Mb}} = -0.159R_1 - 0.085R_2 + 1,262R_2 - 0.520$$

$$R_1 = A582/A525, R_1 = A557/A525, R_1 = A503/A525$$

2.5. Measurement of Hb concentration

A minced muscle sample (4 g) were mixed with 20 mL of Tris (1 mM, pH 8) and homogenised at 3,000 rpm for 60 s (Instrument reference 2.4). The resulting sample was centrifuged at 700 × g for 10 min at 4 °C, and one-tenth of 1 M NaCl was then added to aid in stromal removal before centrifuged at 20,000 × g for 20 min at 4 °C. Low molecular mass components were removed using Amicon Ultra-15 Centrifugal Filter Devices (10 K) (Merck KGaA, Darmstadt, Germany). Using 50 mM Tris, pH 8.0 as the reference, the maximum absorption peak of the bovine haemoglobin (Sigma-Aldrich) standard solution was scanned from 440 to 400 nm, and the concentration of heme protein on a heme basis was calculated using the peak absorbance near 413 nm and a standard curve generated from bovine haemoglobin (Alvarado, et al., 2007).

2.6. Determination of heme iron content

Heme iron content was determined using a method by Taniguchi, et al. (2017) with minor modifications. Briefly, chopped muscle samples (4 g) were mixed with 20 mL of acidified acetone (acetone: water: hydrochloric acid ratio = 45: 4: 1, *v/v/v*), vortexed for 15 s, and then the tubes were incubated in the dark at room temperature for 2 h. The mixture was vacuum filtered through Whatman 42 paper, and the absorbance of the filtrate was measured at 640 nm (Instrument reference 2.3). The level of heme iron in the muscle was determined using the following equations:

$$\text{Hemin } (\mu g \bullet g^{-1} \text{ homogenate}) = A_{640} \times 652 \text{ mg hemin mmol}^{-1} \times \text{total liquid in solution (L)/mass of homogenate used (g)/4.8 L} \bullet \text{mmol}^{-1}/1000\,\mu g \bullet mg^{-1}$$

$$\text{Heme Iron}\left(\mu g \bullet g^{-1}\,\text{homogenate}\right) = \text{hemin}\left(\mu g \bullet g^{-1}\,\text{homogenate}\right) \times 0.0854 \mu g_{Fe}/\mu g_{\text{hemin}}$$

2.7. Determination of non-heme iron content

Non-heme iron content of muscle was determined using the method described by Wang, et al., (2018) with slight modifications. Briefly, 1 g of minced muscle was mixed with 40 μL of 0.39% (*w/v*) $NaNO_2$. The samples were added with 10 mL of a mixture of 20% TCA and 3 M HCl (1:1, *v/v*), the tightly capped test tubes were incubated at 60 °C for 24 h, then the tube was cooled down to room temperature, and analyzed using ICP-OES (Aglient 5110, Agilent Research Laboratories, Santa Clara, California, USA).

2.8. Determination of UV absorption spectrum of haem

Haem extracted using the method described in section 2.3 was subjected to UV absorption spectrum analysis. The phosphate buffer (0.04 M, pH 6.8) was used to dilute the haem pellet to a final concentration of 5 mg/mL. Then, the absorption spectra of the haem solution were measured in the range of 380 to 450 nm using the UV-9000S spectrophotometer. The scanning speed was set at 1,000 nm/min (Wang, et al., 2018).

2.9. Particle size distribution and zeta-potential

The particle size distribution and zeta-potential of the haem samples (5 mg/mL) were determined by using a Litesizer 500 Zeta Potential Analyzer (Anton Paar, Ltd., Austria). Different cuvettes were used for the determination in different modes. The dispersion medium was deionised water (Xia, et al., 2020). All measurements were carried out at room temperature (24 °C).

2.10. Fourier transform infrared (FTIR) spectroscopy

The secondary structure of haem (5 mg/mL) was analysed using VERTEX 70 FTIR spectroscopy (BRUKER, Karlsruhe, Germany). The dispersion medium was deionised water. Scanning was performed using a scanning infrared spectrometer at points between 400 and 4000 cm^{-1}. Subsequently, data between 1600 and 1700 cm^{-1} were extracted for a Gaussian fit using Peakfit 4.12 software (Systat Software Inc., California, USA). The contents of the α-helix, β-sheet, β-turn and random coil were then calculated (Zhao, et al., 2021).

2.11. Myofibrillar protein (MP) extraction

MP of the muscle was isolated using a method as described previously (Xia, et al., 2009), with slight modification. Briefly, 40.00 g muscle without fascia was homogenized by blending for 90 s in a Waring blendor with 160 mL (*w/v*) of isolation buffer (10 mM sodium phosphate, 0.1 M NaCl, 2 mM $MgCl_2$ and 1 mM EGTA, pH 7.0). After centrifuging at 2,000 × g for 15 min at 4 °C, the supernatant was discarded, and the crude MP was obtained. The pellet was washed two more times with 160 mL of the same isolation buffer using the same blending and centrifugation conditions as indicated above. Then, the crude MP was washed and homogenized 3 times with 160 mL 0.1 M NaCl by blending for 90 s, then centrifuged at 2,000 × g for 15 min at 4 °C. In the last wash time, the MP was suspended by 0.1 M NaCl and filtered through four layers of cheesecloth to remove connective tissue. After the pH value was adjusted to 6.00 with 0.1 M HCl, the myofibrillar protein isolate (MPI) was obtained by centrifugation. The protein concentration was determined by the BCA method.

2.12. Sodium dodecyl sulfate–polyacrylamide gel electrophoresis (SDS-PAGE)

The molecular weight (Mw) distribution of Mb, Hb and MP was determined by SDS-PAGE. Mw was determined by using proteins markers (TransGen Biotech, Beijing, China) with molecular weights of 14–120 kDa and 15–250 KDa, according to the Mw of Mb (17.6 KDa) and Hb (64.5 KDa). Electrophoresis was performed at 100 V with a Bio-Rad electrophoresis apparatus (Richmond, CA, USA) with 5% concentrated gel and 12.5% separated gel. The bands were shown by Coomassie Brilliant Blue R-250 (Xia, et al., 2009).

2.13. Myofibrillar protein (MP) oxidation assay

Protein oxidation was determined by measuring the contents of reactive carbonyl (CB) and total sulfhydryl (SH). The contents of CB and SH in MPI were measured with kits (Nanjing Jiancheng Bioengineering Institute, Nanjing, China) following the manufacturer's instructions.

2.14. Lipid oxidation assay

Lipid oxidation was reflected by peroxide value (PV) and malondialdehyde (MDA) content. The PV was determined using a previous method (Liu, et al., 2016; Sun, et al., 2019), with some modifications. Briefly, 1.00 g muscle sample was shredded and homogenized in 10 mL of distilled water and centrifuged at 10, 000 × g for 5 min at 4 °C. Then 5 mL of the supernatant and 3 mL mixture of isooctane/2-propanol (3:1, *v/v*) were mixed and vortexed for 30 s using a VORTEX05 vortex mixer (Shanghai Brave Construction Development Co, Shanghai, China), and centrifuged at 10,000 × g for 5 min at 4 °C. The upper organic phase (400 μL) was mixed with 3 mL mixture of methanol/1-butanol (3:1, *v/v*) solution and 30 μL mixture of 3.94 M ammonium thiocyanate/0.144 M ferrous chloride (1:1, *v/v*) solution. After incubation in the dark for 20 min, the absorbance of the solution was determined at 510 nm using an UV spectrophotometer. PV is calculated using the following formula:

$$PV\left(\text{mmol cumene hydroxide}\,kg^{-1}\,\text{sample}\right) = \frac{C \times 30 \times 50/5}{m \times M}$$

Where C is the concentration of lipid hydroperoxides (μg/mL), m is the weight of chicken breast muscle, and M is the cumene hydroperoxide molar mass (152.19 g/mol).

The MDA content in lipid was determined with kits (Nanjing Jiancheng Bioengineering Institute, Nanjing, China) following the manufacturer's instructions.

2.15. Statistical analysis

Data were statistically analyzed by one-way ANOVA, followed by an LSD test using IBM SPSS Statistics (NY, USA). Graphs were plotted using Origin 2021 software (Massachusetts, USA). The significance threshold for statistical analysis was set at $p < 0.05$. All data given are the mean ± SD (standard deviation) values of three independent experiments.

3. Results and discussion

3.1. Changes in quality indicators during storage of chilled beef

The beef samples stored for 0–4 d showed a significant decrease in pH value ($p < 0.05$), with an increase in pH value for 6 d, which was not different from 4 d ($p > 0.05$). Muscle contains a certain level of glycogen reserves, with a great glycolytic potential, the breakdown of glycogen may further lead to the breakdown of glucose to lactic acid (Purohit, et al., 2015), this could partly explain the decrease in pH value of the beef during storage. The L*-value was the highest on Day 2, but there were no significant changes in the L*-values for 0 d, 1 d and 4 d ($p > 0.05$); the a*-and b*-values for 1 d and 2 d were not significantly different ($p > 0.05$), with the a*-value for 1 d being significantly higher than the other groups ($p < 0.05$), and the b*-value for 2 d being significantly higher than the other groups ($p < 0.05$). Bovine muscle fibres are considered to be red fibres, with at least 40% of their muscle fibres being of the β-red type, and β-red type fibres contain large amounts of mitochondria and Mb, both of which are iron reserves, and this also explains why muscle colour and Mb changes are closely related (Purohit, et al., 2015). Changes in a*-values are attributed to the oxidation of DeoMb and OxyMb and the formation of MetMb (Li, et al., 2018). It was reported that changes in muscle colour were the result of myoglobin oxidation and that myoglobin autoxidation was a trigger for protein oxidation and lipid oxidation (Baron & Andersen, 2002). In terms of WHC, the changes in PL of the sample during storage significantly increased over the whole storage time ($p < 0.05$); DL and CL were significantly higher than the other groups for the 4 d ($p < 0.05$), where the differences in DL between 0 d and 1 d, 1 d and 2 d were not significant ($p > 0.05$). Lindahl, et al. (2010) proposed that the increase in WHC during storage was due to the degradation of tissue skeletal proteins, which eliminated the link between myofibrillar and whole muscle fibres, thus removing the forces that bind water to the muscle fibres. Bao & Ertbjerg. (2019) concluded that oxidative conditions may disrupt the order and integrity of muscle cells and limit the ability of myogenic fibres to absorb water, reducing the WHC of the meat. The relationship between protein oxidation and WHC was demonstrated by the increased formation of carbonyl compounds, decreased formation of sulfhydryl compounds (Fig. 2 and Fig. 3b).

3.2. Spin-Spin relaxation time (T_2)

The content and distribution of water in the muscle were studied by measuring the proton spin–spin relaxation time (T_2) using low-field NMR (LF-NMR). The bound water (T_{21}, 1–10 ms), immobilized water (T_{22}, 10–100 ms) and free water (T_{23}, 100–1000 ms) were considered as the three relaxation T_2 water populations (Li, et al., 2018). As shown in Fig. 1a, there were three groups of water in the meat, but the relaxation times were different from those of the previous studies (Li, et al., 2018; Li, et al., 2014). The area under each peak represents the water population, with minor components between 0.1 and 0.5 ms and between 0.5 and 4, possibly representing bound water (T_{21}) and immobilized water (T_{22}). The major component between 10 and 10000 ms reflects free water (T_{23}). The peak area reflects the amount of water in the muscle-with a gradual decrease in water content with increasing storage time (Fig. 1b). Also, as shown in Fig. 1c, the changes in the ratios of T_{21}, T_{22}, and T_{23} with storage time had little effect on the change in T_{21}. T_{22} and T_{23} reflect water located within a highly organized intra-myofibrillar protein matrix, and the change in water distribution throughout the storage period showed a decrease in fixed water and an increase in free water, which is consistent with a previous report (Chen, et al., 2015). T_{22} corresponds to water located within a highly organized myofibrillar protein matrix including actin and myosin filament structures (Li, et al., 2018). This change in fixed and free water in the muscle during storage may be caused by the water transfer between fibers and changes of hydrogen bonds between protein and water, and protein oxidation is considered to be a potential producer. Notably, oxidation of MP resulted in a certain degree of conversion of fixed water to free water, leading to a loss of drip water from the muscle during storage (Li, et al., 2014), which was verified by the change in WHC (Table 1).

3.3. Changes in contents of myoglobin (Mb) and haemoglobin (Hb)

As shown in Fig. 2a and b, the proportion of DeoMb and OxyMb significantly decreased ($p < 0.05$) and the proportion of MetMb significantly increased ($p < 0.05$) throughout the storage period. Normally, the increase of MetMb content can be observed during freezing or cold storage of many dark-coloured meats, indicating that ferrous myoglobin (DeoMb and OxyMb) may undergo oxidation during storage to form

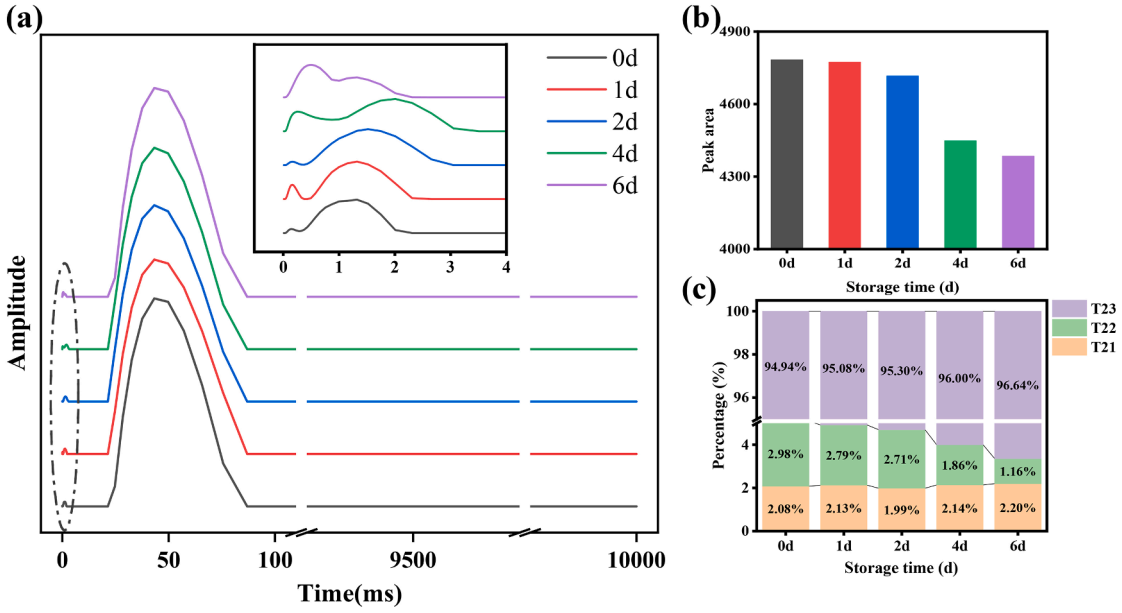

Fig. 1. Low-field NMR to determine the state of water distribution in muscle. (a) Distribution of low-field NMR T2 relaxation times during muscle storage; (b) Distribution of the peak areas of low-field NMR spectra during muscle storage; (c) Distribution of the differences in proton spin–spin relaxation times (T_{21}, T_{22}, T_{23}) in low-field NMR during muscle storage. T_{21} indicates bound water; T_{22} indicates immobilized water; T_{23} indicates free water.

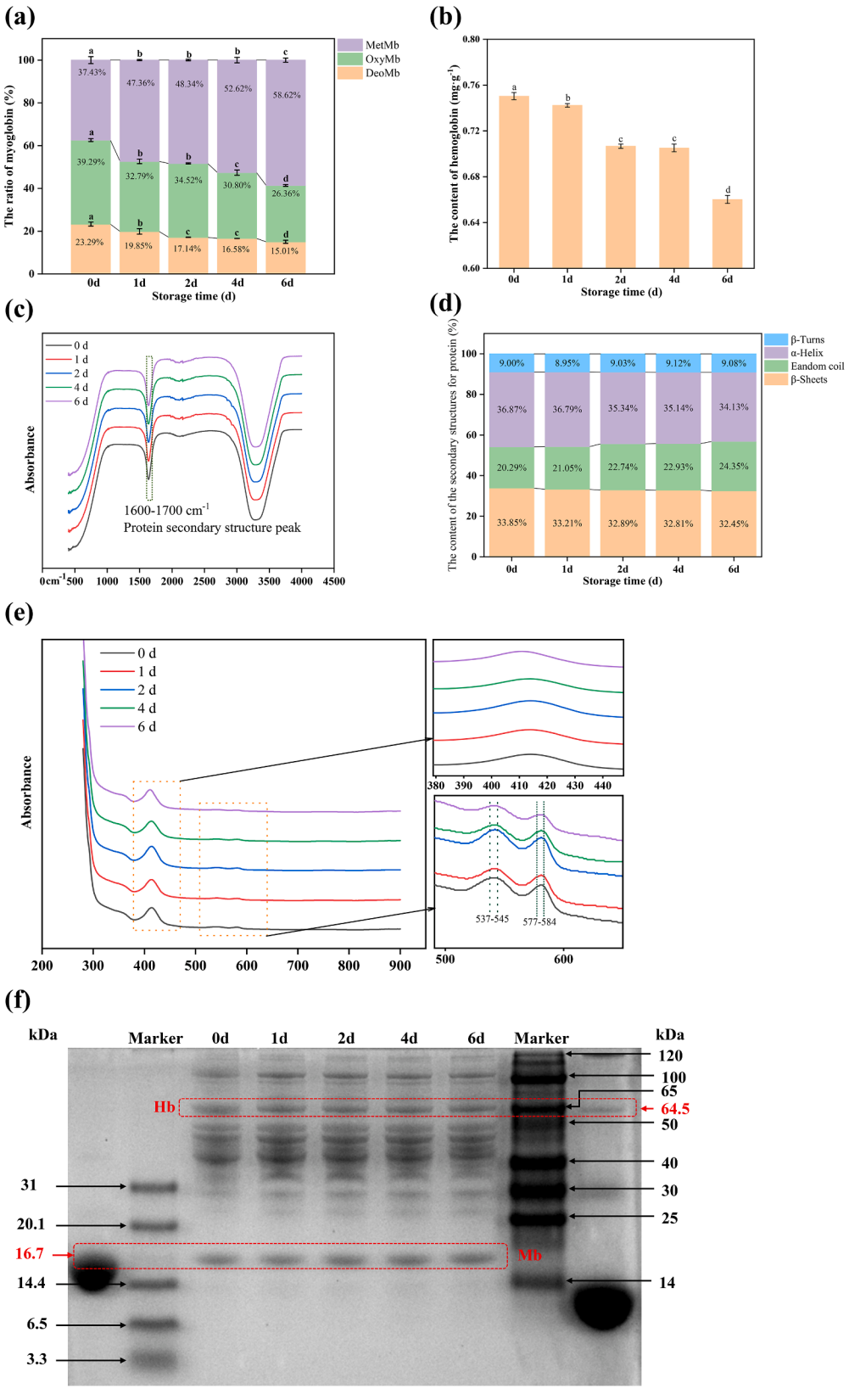

Fig. 2. Morphological and structural analysis of myoglobin (Mb) and haemoglobin (Hb). (a) Relative proportions of the redox forms of Mb (DeoMb, OxyMb and MetMb) formed in bovine muscle during storage period. (b) Effect of storage time on the total Mb concentration in bovine muscle. (c) Changes in FTIR spectroscopy (400–4000 nm) of bovine muscle haem during storage. (d) Changes in the relative contents of bovine muscle haem secondary structures (α-helix, β-sheets, β-turns and random coil) during storage. (e) Changes in the absorption spectra of bovine muscle haem in the soret region (280–900 nm) during storage. (f) SDS-PAGE of haem (Hb and Mb) in muscle at different storage times. Mb indicates myoglobin, Hb indicates haemoglobin. DeoMb, OxyMb and MetMb represent deoxymyoglobin, oxymyoglobin, and metmyoglobin respectively. Molecular weight: Hb, 64.5 kDa; Mb, 16.7 kDa; Different letters (a-d) are significantly different ($p < 0.05$).

ferric MetMb (Wongwichian, et al., 2015). Oxidation typically starts once the muscle has been divided in fresh meat, ferric MetMb can be reduced to DeoMb and OxyMb due to the presence of the deoxymyoglobin-reducing enzyme (MRE) system. Thus, no rapid accumulation of metmyoglobin was observed in the 0 d samples of beef after slaughter. However, the activity of MRE decreased when the meat was aged or was refrigerated and the rate of oxidation of DeoMb and OxyMb accelerated, which led to the accumulation of DeoMb (Li, et al., 2018).

The Hb content was found to significantly decrease throughout the storage period ($p < 0.05$). The main source of Hb in the muscle is the

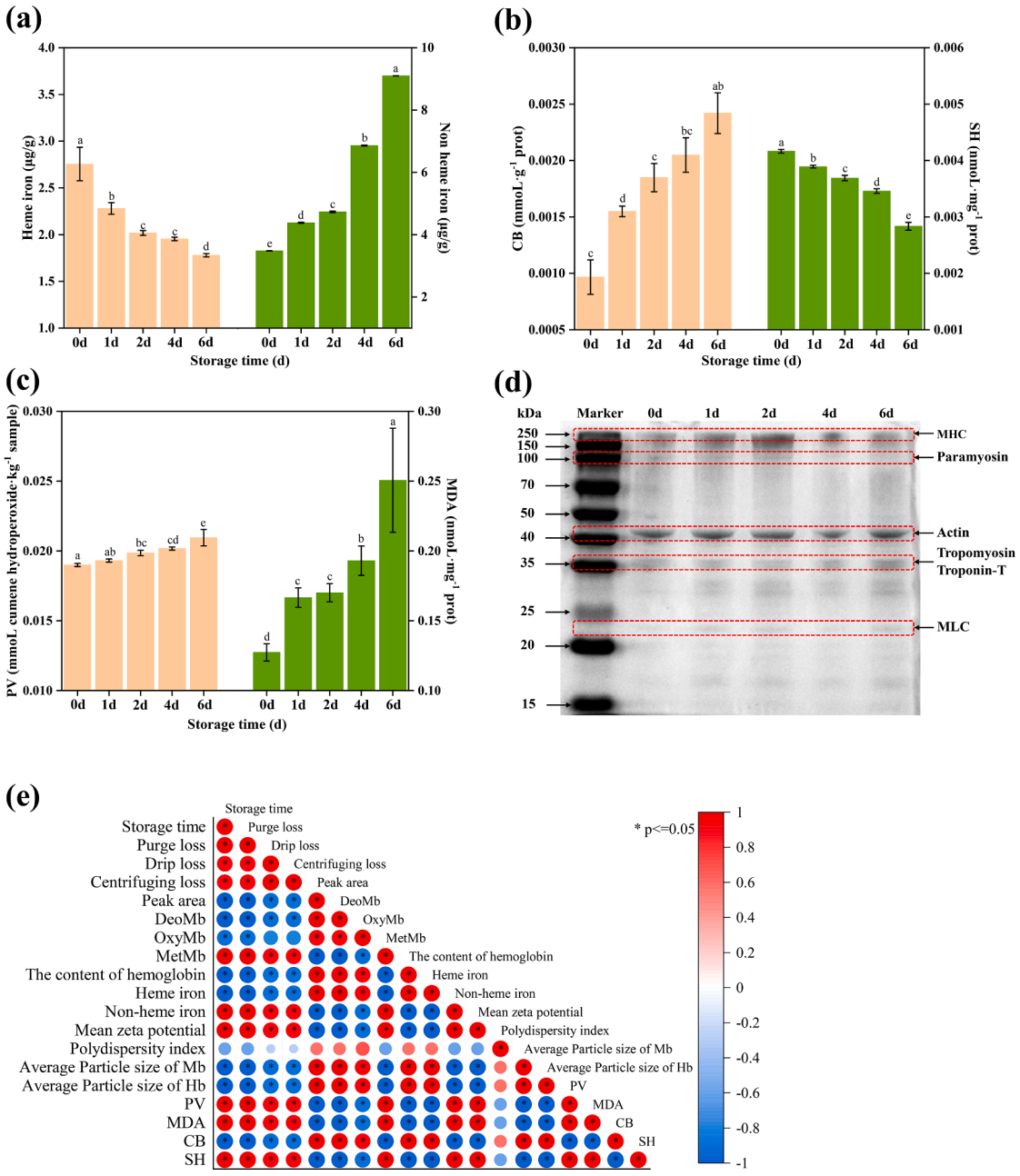

Fig. 3. Analyses of iron ion status, protein and lipid oxidation,and their correlations with water holding capacity. (a) Changes in the heme iron (left) and non-heme iron (right) content of bovine muscle during storage. (b) Changes in the contents of carbonyl (CB) (left) and sulfhydryl (SH) (right) of protein oxidation products. (c) Changes in the peroxide value (PV) (left) and malondialdehyde (MDA) (right) content of lipid oxidation products. (d) SDS-PAGE of myoglobin proteins in muscle at different storage times. (e) Correlation matrix heat maps of meat quality attributes and water holding capacity features during storage of bovine muscles. Molecular weight: Myosin light chain (MLC), 16–25 kDa; Troponin-T, 35 kDa; Tropomyosin, 36 kDa; Actin, 43 kDa; Paramyosin, 100 kDa; Myosin heavy chain (MHC), 220 kDa. Mb indicates myoglobin, Hb indicates haemoglobin. DeoMb, OxyMb and MetMb represent deoxymyoglobin, oxymyoglobin, and metmyoglobin respectively. Different letters (a-e) indicate significant differences between samples ($p < 0.05$). "*" indicates a significant correlation at $p < 0.05$. Red indicates positive correlation, blue indicates negative correlation, the darker the colour the higher the correlation.

residue of blood at the time of slaughter, which is retained in the blood vessels or permeated into the tissues by ruptured vessels due to carcass damage. Hb in the meat is very unstable and carries a high level of oxygen, making it more susceptible to oxidation and structural damage (Alvarado, et al., 2007; Thiansilakul, et al., 2012). Gel electrophoresis showed the bands of haemoglobin and myoglobin at 64.5 kDa and 16.7 kDa (Fig. 2f), indicating that they were present in the muscle. Haem has high protein and lipid pro-oxidative capacities, particularly metmyoglobin, through several mechanisms, such as hydroperoxide catabolism and the ability to act as a free radical due to its conversion to the ferril or preferred form (Wongwichian, et al., 2015). In addition, during the oxidation of deoxymyoglobin or oxymyoglobin, superoxide anions and hydrogen peroxide are produced, and further reacts with free iron to form •OH, while haem is more sensitive to the destruction of haem, which releases more iron and induces the production of more •OH (Richards, et al., 2007). The •OH can penetrate the hydrophobic protein and lipid regions of the muscle, hence facilitating protein and lipid oxidation (Wongwichian, et al., 2015).

Table 1
Changes in pH value, color and WHC of beef during storage.

Quality evaluation	0 d	1 d	2 d	4 d	6 d
pH	6.50 ± 0.05^{a}	5.82 ± 0.03^{b}	5.69 ± 0.02^{c}	5.53 ± 0.03^{d}	5.57 ± 0.02^{d}
L*	32.50 ± 0.51^{a}	33.28 ± 1.36^{a}	35.07 ± 1.65^{b}	32.95 ± 1.34^{ac}	30.94 ± 1.86^{d}
a*	17.76 ± 0.67^{a}	20.76 ± 1.30^{b}	20.45 ± 1.23^{b}	15.66 ± 1.45^{c}	12.42 ± 1.43^{d}
b*	2.24 ± 0.36^{a}	5.38 ± 0.50^{b}	5.68 ± 0.84^{b}	4.41 ± 0.81^{c}	3.24 ± 0.65^{d}
Purge loss (%)	0.35 ± 0.02^{a}	0.59 ± 0.01^{b}	0.64 ± 0.04^{b}	0.79 ± 0.07^{c}	1.02 ± 0.09^{d}
Drip loss (%)	2.29 ± 0.19^{a}	2.76 ± 0.09^{ab}	3.18 ± 0.17^{b}	6.14 ± 0.25^{c}	4.38 ± 0.88^{d}
Centrifuging loss (%)	9.69 ± 0.73^{a}	12.08 ± 0.27^{b}	13.53 ± 0.42^{c}	16.90 ± 0.94^{d}	15.30 ± 0.44^{e}

Note: 0 d, 1 d, 2 d, 4 d and 6 d indicate beef stored at 4 °C for 0, 1, 2, 4 and 6 days respectively. Means within the same row with different superscript letters (a-e) are significantly different ($p < 0.05$). L* indicates lightness, a* indicates redness, and b* indicates yellowness.

Table 2
Effects of storage time on the average particle size, polydispersity index and zeta-potential of haem.

Storage time (d)	Mean zeta potential (mV)	Polydispersity index (PDI)	Average Particle size of Mb (nm)	Average Particle size of Hb (nm)
0	−7.5231 ± 0.6303^{a}	40.6351 ± 7.3625^{a}	588.0385 ± 8.8592^{a}	9622.7737 ± 663.4815^{a}
1	−6.8440 ± 1.7691^{a}	32.6015 ± 9.2784^{a}	559.1139 ± 10.2516^{b}	6459.6037 ± 2280.6309^{b}
2	−5.3188 ± 2.2713^{a}	34.6197 ± 2.9393^{a}	492.9514 ± 28.0410^{c}	4866.8969 ± 1648.5459^{bc}
4	−2.6846 ± 0.9914^{b}	38.3419 ± 15.4174^{a}	480.147 ± 18.8856^{c}	3839.5335 ± 953.9103^{c}
6	−2.5593 ± 0.7468^{b}	28.4283 ± 3.2138^{a}	475.3618 ± 14.3095^{c}	3222.0169 ± 847.2869^{c}

Note: Mb indicates myoglobin, Hb indicates haemoglobin. Means within the same column with different superscript letters (a-c) are significantly different ($p < 0.05$).

3.4. Particle size and zeta-potential distribution

As shown in Table 2, the zeta potential decreased with increasing storage time, but no significant differences were observed at 0 d, 1 d and 2 d ($p > 0.05$). Zeta potential indicates the near-surface or surface charge of the suspended particles, and the oxidation unfolded the haem agglomerates, exposing more of the buried charged $Fe^{2+/3+}$ inside the porphyrin heme to the protein surfaces, resulting in a rearrangement of the surface charge of haem and the exposed iron atoms to move directionally, leading to an increase in the zeta potential of the suspended haem particles (Xia, et al., 2020). Additionally, the conversion of the iron atoms in the centre of the porphyrin ring from Fe^{2+} to Fe^{3+} led to an increase in the zeta potential (Lund, et al., 2011). No significant differences were observed in the polydispersity index (PDI) throughout the storage period ($p > 0.05$), with the smallest PDI observed at 6 d. The average particle size of Mb and Hb decreased with increasing storage time, with a 19.21% reduction in Mb particle size and a 66.51% reduction in Hb particle size. The particle size of the suspended particle reflects the aggregation state of the particles, and the decrease in particle size indicates the depolymerisation and degradation of the molecular groups. As shown in Fig. 2b, the Hb content was found to decrease during the storage, which is consistent with the result in Hb particle size.

3.5. Changes in absorption spectra in the soret region and secondary structure of haem

As shown in Fig. 2e, the strong peaks in the soret region were observed at 414 nm and 411 nm, reported to be the absorption peaks for myoglobin (Wang, et al., 2018), and the intense absorption peak gradually decreased with storage time. The soret bands were a porphyrin compound with a characteristic absorption peak in the UV–visible 420 nm region, mainly produced by the interaction between haem and apomyoglobin, hence it may reflect the unfolding of haem (Wang, et al., 2018). The decrease in intense peak can indicate destruction of haem, or separation of the porphyrin fraction from the bead protein (Baron & Andersen, 2002). Mb underwent degradation from 0 to6 d of storage. Thiansilakul, et al., (2012) reported that Hb had a Soret peak at 420 nm and two additional peaks at 530 and 570 nm. Richards et al., (2003) found that fully deoxygenated Hb showed a single peak near 560 nm, while fully oxygenated Hb showed two sharp peaks near 576 and 540 nm, forming a deep valley. As shown in Fig. 2e, two sharp peaks were observed at 537–545 nm and 577–584 nm, with a deep valley at 560 nm. Also, the height of both spikes and troughs decreased with increasing storage time, indicating a decrease in deoxyhaemoglobin content and an increase in oxyhaemoglobin level.

In addition, the secondary structure of haem was further analysed by FTIR spectroscopy (Fig. 2c). The secondary structure of haem was determined by intercepting the region of amide I band (1700–1600 cm^{-1}) from the raw FTIR signal (Zhao, et al., 2021). The infrared spectrum bands mainly reflect the C-double bond O stretching vibration and the hydrogen bonding between the C-double bond O and N—H groups (Stani, et al., 2020). The protein secondary structures have different hydrogen bonds, and therefore their absorption peak positions in the amide I band also differ. The main secondary structures of proteins are α-helix, β-sheets, β-turns and random coil (Xia, et al., 2020), and the overall transition of peak attribution in amide I is as follows: β-sheet (1700–1682 cm-1), β-turn (1681–1664 cm^{-1}), α-helix (1663–1646 cm^{-1}), random coil (1645–1637 cm^{-1}) and β-sheet (1636–1615 cm^{-1}) (Zhao, et al., 2021). A significant decrease in the level of α-helix (36.87% to 34.13%) and a significant increase in the content of random coil (20.29% to 24.35%) were found (Fig. 2d), indicating a disruption of the secondary structure of myoglobin, causing chaos in the structures and verifying that haem degradation occurred during storage. Notably, there were no significant changes in the contents of β-turning angles and β-folding in the secondary structure.

3.6. Changes in heme iron and non-heme iron contents

Generally, heme iron content gradually decreased with increasing storage time ($p < 0.05$, Fig. 3a). The heme iron content (initially 2.755 μg/g) decreased by 35.53% after 6 d of storage, whereas the non-heme iron content increased from 9.130 μg/g to 18.495 μg/g ($p < 0.05$). The decrease in haem iron content was inversely proportional to the non-haem iron content. The decrease in haem iron content may be because some porphyrin rings have been destroyed during storage period, and free iron was released from the haem (Grunwald & Richards, 2012). A higher content of soluble haem pigment was found in fresh muscle, and the higher the haem extraction rate, the extractability of haem pigments was reduced with increasing storage time by interactions between haem pigments and muscle components, such as the interaction of haem with myofibrillar proteins and cellular membranes (Chaijan, et al., 2007). The heme degradation could be reflected by an increase of non-heme iron content (Chen, et al., 2021). As shown in Fig. 3a, the non-haem iron content significantly increased during storage ($p < 0.05$). In addition to haem (haemoglobin and myoglobin), iron was also present in the insoluble fraction of muscle, ferritin, iron-sulphur protein, mitochondrial iron-containing enzymes and low molecular weight fractions (Angeli, et al., 2017; Delanghe & Langlois, 2001). Therefore, muscle cell apoptosis and tissue degradation may result in the release of iron from

these fractions as storage time increases, leading to an increase in non-haem iron content (Chen, et al., 2021). The released iron ions may induce the production of hydroxyl radicals, and this free iron can act as a pro-oxidant to enhance protein and lipid oxidation (Zhang, et al., 2021).

3.7. Protein and lipid oxidation

The depot or intermuscular lipids are generally stored in specialized connective tissues, whereas tissue lipids are integrated into and widely distributed throughout the muscle tissues (Love & Pearson, 1971). Peroxide value (PV) and malondialdehyde (MDA) are the most frequently used indicators for lipid oxidation in meat (Al-Dalali, et al., 2022). As shown in Fig. 3c, the levels of PV and MDA significantly increased at the beginning and end of the storage period ($p < 0.05$). When hydrogen atoms in unsaturated fatty acids are seized by free radicals during storage of muscle, the free radicals become non-radicals and the fatty acids become free radicals, called lipid radicals (L·). During this process many primary and secondary by-products are produced, e.g. 4-hydroxynonenal and MDA. The contents of PV and MDA significantly increased ($p < 0.05$, Fig. 3c), indicating the enhanced lipid oxidation in bovine muscle during refrigeration. Ferric haem pigments are thought to be the main pro-oxidants in tissue lipid oxidation. Haem and lipid oxidation are interrelated, and ferric haem is thought to promote lipid oxidation, with the resulting oxidation destroying haem and promoting the detachment of iron ions from the haem structure (Baron & Andersen, 2002). Non-haem iron can also act as a pro-oxidant in meat through the Fenton reaction (Love & Pearson, 1971). Fenton reaction and the metal-catalyzed Haber-Weiss reaction produce hydroxyl radicals from hydrogen peroxide, and the main pathways of ·OH radical production are shown in the equation below:

1. Fe-dependent decomposition of H_2O_2 (Fenton reaction).

$$Fe^{2+} + H_2O_2 \rightarrow Fe^{3+} + \bullet OH + OH^-$$

$$Fe^{2+} + H_2O_2 \rightarrow \text{ferryl} \rightarrow Fe^{3+} + \bullet OH + OH^-$$

2. Metal-catalyzed Haber-Weiss reaction or superoxide-driven Fenton reaction.

$$Fe^{3+} + O_{2^-} \rightarrow Fe^{2+} + O_2$$

$$Fe^{2+} + H_2O_2 \rightarrow Fe^{3+} + \bullet OH + OH^-$$

Protein oxidation leads to a variety of changes in proteins, including amino acids, formation of protein-polymers, loss of solubility, reduction of the thiol groups, and an increase in carbonyl groups (Al-Dalali, et al., 2022). As shown in Fig. 3b, the protein carbonyl content increased from 0.00096 ± 0.00065 to 0.00242 ± 0.00018 mmoL·mg^{-1} prot ($p < 0.05$) and the sulfhydryl content decreased from 0.00416 ± 0.00003 to 0.00283 ± 0.00003 mmoL·mg^{-1} ($p < 0.05$). Muscle contains the pro-oxidative Mb or Hb, which has been shown to trigger protein oxidation. When the reductases in meat are depleted as a result of slaughter, metmyoglobin may accumulate in the meat and, by reaction with H_2O_2, form hypervalent Mb-species perferrylmyoglobin and ferrylmyoglobin (peroxidation cycle) (Lund, et al., 2011). In the study, the proportion of metmyoglobin increased with increasing storage time (Fig. 2a). The reaction between iron and H_2O_2 (Fenton reaction) is regarded as a common source of highly reactive hydroxyl radicals (•OH). The increase in non-heme content resulted in an enhanced Fenton reaction (Fig. 3a). The oxidation of MP in model systems and muscle foods has been linked to the participation of Fe^{3+} as a required initiation factor (Al-Dalali, et al., 2022). The involvement of transition metals generally leads to the formation of protein carbonyl groups and protein hydroperoxides, while cross-linking has been described as formation of disulfide and dityrosine through the loss of cysteine and tyrosine residues from particular amino acids (Zhang, et al., 2019). Lipid and protein oxidation processes are unlikely to occur independently, with lipid oxidation occurring more rapidly, and therefore lipid-derived free radicals and hydroperoxides are more likely to promote protein oxidation. Proteins that are abundant in muscle cells are affected by oxidative processes, particularly myogenic fibronectin (Lund, et al., 2011). As shown in Fig. 3e, MP mainly contained myosin heavy chain (MHC) (200 kDa) and actin (43 kDa). Little change in the number of electrophoretic bands was observed, indicating that the composition of myogenic fibrillar proteins was barely affected, and the main protein that was degraded was MHC. Oxidation of myogenic fibronectin led to an unfolding of the protein structure and an increase in protein–protein interactions, ultimately altering the WHC of MP (Yulong & Per, 2018).

3.8. Correlation between physicochemical properties and WHC of Mb and Hb

As shown in Fig. 3e, there were significant positive correlations ($p < 0.05$) between muscle WHC (purge loss, drip loss and centrifuging loss) and the proportion of metmyoglobin, non-haem iron content, protein and lipid oxidation, and significant positive correlations ($p < 0.05$) were observed between the proportion of metmyoglobin, non-haem iron content, protein and lipid oxidation, implying that the release of metmyoglobin and haem iron may promote the release of MP and lipid oxidation, and thus decrease WHC. Furthermore, these processes were mutually reinforcing and not independent of each other.

4. Conclusions

The accumulation of metmyoglobin and release of non-haem iron, accompanied by an increase in the degree of lipid and protein oxidation, caused muscle juice loss during refrigeration of bovine muscle. Furthermore, the oxidation and degradation of Hb and Mb were found to promote muscle juice loss. This provides new ways of improving the water holding capacity of beef, including inhibiting myoglobin oxidation during muscle storage and bleeding the carcass sufficiently at slaughter to reduce carcass blood residues.

CRediT authorship contribution statement

Jun Liu: Conceptualization, Data curation, Formal analysis, Investigation, Methodology, Resources, Validation, Visualization, Writing – original draft, Writing – review & editing. **Dunhua Liu:** Conceptualization, Formal analysis, Funding acquisition, Investigation, Project administration, Supervision, Visualization. **Anran Zheng:** Investigation. **Qin Ma:** Writing – review & editing.

Declaration of Competing Interest

The authors declare that they have no known competing financial interests or personal relationships that could have appeared to influence the work reported in this paper.

Acknowledgments

The authors would like to thank Associate Professor Yanli Fan for providing apparatus support. We're especially grateful for Xiaoyi Mao, Caixia Men, Yuanyuan Zhang, Xiaolu Zhao and all people participating in the preparations and analysis of this study.

Funding

This study was financially supported by the Ningxia Natural Science Foundation (2021AAC03013, 2022AAC02021).

Data availability statement

Not applicable.

References

Al-Dalali, S., Li, C., & Xu, B. (2022). Effect of frozen storage on the lipid oxidation, protein oxidation, and flavor profile of marinated raw beef meat. *Food Chemistry, 376*, Article 131881. https://doi.org/10.1016/j.foodchem.2021.131881

Alvarado, C. Z., Richards, M. P., O Keefe, S. F., & Wang, H. (2007). The effect of blood removal on oxidation and shelf life of broiler breast meat. *Poultry Science*, 86, 156-161. https://doi.org/10.1093/ps/86.1.156.

Angeli, J., Shah, R., Pratt, D. A., & Conrad, M. (2017). Ferroptosis inhibition: Mechanisms and opportunities. *Trends in Pharmacological Sciences, 38*, 489–498. https://doi.org/10.1016/j.tips.2017.02.005

Bao, Y., & Ertbjerg, P. (2019). Effects of protein oxidation on the texture and water-holding of meat: A review. *Critical Reviews in Food Science and Nutrition, 59*, 3564–3578. https://doi.org/10.1080/10408398.2018.1498444

Baron, C. P., & Andersen, H. J. (2002). Myoglobin-induced lipid oxidation. *A review. J. Agric. Food Chem., 50*, 3887–3897. https://doi.org/10.1021/jf011394w

Chaijan, M., Benjakul, S., Visessanguan, W., Lee, S., & Faustman, C. (2007). The effect of freezing and aldehydes on the interaction between fish myoglobin and myofibrillar proteins. *J. Agric. Food Chem., 55*, 4562–4568. https://doi.org/10.1021/jf070065m

Chen, C., Guo, Z., Ma, G., Ma, J., Zhang, Z., Yu, Q., & Han, L. (2021). Lysosomal Fe2+ contributes to myofibrillar protein degradation through mitochondrial-dysfunction-induced apoptosis. *LWT, 143*, Article 111197. https://doi.org/10.1016/j.lwt.2021.111197

Chen, L., Zhou, G., & Zhang, W. (2015). Effects of high oxygen packaging on tenderness and water holding capacity of pork through protein oxidation. *Food and Bioprocess Technology, 8*, 2287–2297. https://doi.org/10.1007/s11947-015-1566-0

Delanghe, J. R., & Langlois, M. R. (2001). Hemopexin: A review of biological aspects and the role in laboratory medicine. *Clinica Chimica Acta, 312*, 13–23. https://doi.org/10.1016/S0009-8981(01)00586-1

Grunwald, E. W., & Richards, M. P. (2006). Mechanisms of heme protein-mediated lipid oxidation using hemoglobin and myoglobin variants in raw and heated washed muscle. *J. Agric. Food Chem., 54*, 8271–8280. https://doi.org/10.1021/jf061231d

Grunwald, E. W., & Richards, M. P. (2012). Effects of hemopexin on hemin and hemoglobin-mediated lipid oxidation in washed fish muscle. *LWT - Food Science and Technology, 46*, 412–418. https://doi.org/10.1016/j.lwt.2011.12.007

Hanan, T., & Shaklai, N. (1995). The role of H_2O_2-generated myoglobin radical in crosslinking of myosin. *Free Radical Research, 22*, 215–227. https://doi.org/10.3109/10715769509147541

Li, X., Wei, X., Wang, H., Zhang, C., & Mehmood, W. (2018). Relationship between protein denaturation and water holding capacity of pork during postmortem ageing. *Food Biophysics, 13*, 18–24. https://doi.org/10.1007/s11483-017-9507-2

Li, Y., Jia, W., Zhang, C. H., Li, X., Wang, J. Z., Zhang, D. Q., & Mu, G. F. (2014). Fluctuated low temperature combined with high-humidity thawing to reduce physicochemical quality deterioration of beef. *Food and Bioprocess Technology, 7*, 3370–3380. https://doi.org/10.1007/s11947-014-1337-3

Lindahl, G., Lagerstedt, Å., Ertbjerg, P., Sampels, S., & Lundström, K. (2010). Ageing of large cuts of beef loin in vacuum or high oxygen modified atmosphere - Effect on shear force, calpain activity, desmin degradation and protein oxidation. *Meat Science, 85*, 160–166. https://doi.org/10.1016/j.meatsci.2009.12.020

Liu, F., Zhu, Z., Ma, C., Luo, X., Bai, L., Decker, E. A., Gao, Y., Mcclements, D. J., & AU. (2016). Fabrication of concentrated fish oil emulsions using dual-channel microfluidization: Impact of droplet concentration on physical properties and lipid oxidation. *Journal of Agricultural and Food Chemistry*, 64, 9532-9541. https://doi.org/10.1021/acs.jafc.6b04413.

Love, J. D., & Pearson, A. M. (1971). Lipid oxidation in meat and meat products - a review. *Journal of the American Oil Chemists' Society, 48*, 547–549. https://doi.org/10.1007/BF02544559

Lund, M., Heinonen, M., Baron, C., & Estevez, M. (2011). Protein oxidation in muscle foods: A review. *Molecular Nutrition & Food Research, 55*, 83–95. https://doi.org/10.1007/BF02544559

Pearce, K. L., Rosenvold, K., Andersen, H. J., & Hopkins, D. L. (2011). Water distribution and mobility in meat during the conversion of muscle to meat and ageing and the impacts on fresh meat quality attributes — a review. *Meat Science, 89*, 111–124. https://doi.org/10.1016/j.meatsci.2011.04.007

Purohit, A., Singh, R., Kerr, W., & Mohan, A. (2015). Effects of heme and nonheme iron on meat quality characteristics during retail display and storage. *Journal of Food Measurement and Characterization, 9*, 175–185. https://doi.org/10.1007/s11694-015-9222-y

Rhee, K. S., & Ziprin, Y. A. (1987). Lipid oxidation in retail beef, pork and chicken muscles as affected by concentrations of heme pigments and nonheme iron and microsomal enzymic lipid peroxidation activity. *Journal of Food Biochemistry, 11*, 1–15. https://doi.org/10.1111/j.1745-4514.1987.tb00109.x

Richards, M. P., Nelson, N. M., Kristinsson, H. G., Mony, S. S. J., Petty, H. T., & Oliveira, A. C. M. (2007). Effects of fish heme protein structure and lipid substrate composition on hemoglobin-mediated lipid oxidation. *J. Agric. Food Chem., 55*, 3643–3654. https://doi.org/10.1021/jf0628633

Stani, C., Vaccari, L., Mitri, E., & Birarda, G. (2020). FTIR investigation of the secondary structure of type I collagen: New insight into the amide III band. *Spectrochimica Acta Part A: Molecular and Biomolecular Spectroscopy, 229*, Article 118006. https://doi.org/10.1016/j.saa.2019.118006

Sun, X., Guo, X., Ji, M., Wu, J., Zhu, W., Wang, J., … Zhang, Q. (2019). Preservative effects of fish gelatin coating enriched with CUR/βCD emulsion on grass carp (Ctenopharyngodon idellus) fillets during storage at 4 °C. *Food Chemistry, 272*, 643–652. https://doi.org/10.1016/j.foodchem.2018.08.040

Tang, J., Faustman, C., & Hoagland, T. A. (2004). Krzywicki revisited: Equations for spectrophotometric determination of myoglobin redox forms in aqueous meat extracts. *Journal of Food Science, 69*, C717–C720. https://doi.org/10.1111/j.1365-2621.2004.tb09922.x

Taniguchi, C. N., Dobbs, J., & Dunn, M. A. (2017). Heme iron, non-heme iron, and mineral content of blood clams (Anadara spp.) compared to Manila clams (V. Philippinarum), Pacific oysters (C. Gigas), and beef liver (B. Taurus). *Journal of Food Composition and Analysis, 57*, 49–55. https://doi.org/10.1016/j.jfca.2016.12.018

Thiansilakul, Y., Benjakul, S., Grunwald, E. W., & Richards, M. P. (2012). Retardation of myoglobin and haemoglobin-mediated lipid oxidation in washed bighead carp by phenolic compounds. *Food Chemistry, 134*, 789–796. https://doi.org/10.1016/j.foodchem.2012.02.182

Valenzuela, C., López de Romaña, D., Olivares, M., Morales, M. S., & Pizarro, F. (2009). Total iron and heme iron content and their distribution in beef meat and viscera. *Biological Trace Element Research, 132*, 103–111. https://doi.org/10.1007/s12011-009-8400-3

Wang, H., Song, Y., Liu, Z., Li, M., Zhang, L., Yu, Q., … Wei, J. (2020). Effects of iron-catalyzed and metmyoglobin oxidizing systems on biochemical properties of yak muscle myofibrillar protein. *Meat Science, 166*, Article 108041. https://doi.org/10.1016/j.meatsci.2019.108041

Wang, Z., He, Z., Gan, X., & Li, H. (2018). Interrelationship among ferrous myoglobin, lipid and protein oxidations in rabbit meat during refrigerated and superchilled storage. *Meat Science, 146*, 131–139. https://doi.org/10.1016/j.meatsci.2018.08.006

Wongwichian, C., Klomklao, S., Panpipat, W., Benjakul, S., & Chaijan, M. (2015). Interrelationship between myoglobin and lipid oxidations in oxeye scad (Selar boops) muscle during iced storage. *Food Chemistry, 174*, 279–285. https://doi.org/10.1016/j.foodchem.2014.11.071

Xia, M., Chen, Y., Ma, J., Yin, X., Li, Z., Xiong, G., … Zhou, Y. (2020). Low frequency magnetic fields modification on hydrogen peroxide oxidized myoglobin-isolate and mechanisms underlying the chain reaction process. *Food Chemistry, 312*, Article 126069. https://doi.org/10.1016/j.foodchem.2019.126069

Xia, X., Kong, B., Qian, L., & Jing, L. (2009). Physicochemical change and protein oxidation in porcine longissimus dorsi as influenced by different freeze-thaw cycles. *Meat Science, 83*, 239–245. https://doi.org/10.1016/j.meatsci.2009.05.003

Yulong, B., & Per, E. (2018). Effects of protein oxidation on the texture and water-holding of meat: A review. *Critical Reviews in Food Science & Nutrition, 59*(22), 3564–3578. https://doi.org/10.1080/10408398.2018.1498444

Zhang, M., Wang, D., Xu, X., & Xu, W. (2019). Comparative proteomic analysis of proteins associated with water holding capacity in goose muscles. *Food Research International, 116*, 354–361. https://doi.org/10.1016/j.foodres.2018.08.048

Zhang, M., Yan, W., Wang, D., & Xu, W. (2021). Effect of myoglobin, hemin, and ferric iron on quality of chicken breast meat. *Anim Biosci, 34*, 1382–1391. https://doi.org/10.5713/ajas.20.0529

Zhao, J., Cui, J., Chen, R., Tang, Z., Tan, Z., Jiang, L., & Liu, F. (2021). Real-time in-situ quantification of protein secondary structures in aqueous solution based on ATR-FTIR subtraction spectrum. *Biochemical Engineering Journal, 176*, Article 108225. https://doi.org/10.1016/j.bej.2021.108225

Zheng, H., Han, M., Yang, H., Xu, X., & Zhou, G. (2018). The effect of pressure-assisted heating on the water holding capacity of chicken batters. *Innovative Food Science & Emerging Technologies, 45*, 280–286. https://doi.org/10.1016/j.ifset.2017.11.011